Journal of Medicine and Biology

Research Article | Vol 2 Iss 2

Measured and Calculated Out-of-Field Dose Using Pinpoint Ionization Chamber Detector

Ahmed M Abdelaal[1*], Ehab M Attalla[2,3] and Wael M Elshemey[4]

[1]Radiotherapy Department, Nasser Institute, Cairo, Egypt

[2]National Cancer Institute, Cairo University, Egypt,

[3]Cancer Children Hospital, Cairo, Egypt

[4]Biophysics Department, Cairo University, Egypt

[*]**Corresponding author:** Ahmed M Abdelaal, Radiotherapy Department, Nasser Institute, Cairo, Egypt, Tel: 000201280164166; Email: mosa_science2010@yahoo.com

Abstract

This work aims to provide a comparison between measured and calculated out-of-field dose using Pinpoint ionization chamber detector. This detector is used in radiation dosimetery in radiotherapy. The comparison utilizes important dosimetric parameters such as field size (from 10 × 10 cm^2 to 30 × 30 cm^2) and depth (from 1.5 cm to 10 cm) at two different energies (6 MV and 15 MV) and two different collimator angles (0° and 90°). The change in measured and calculated out-of-field dose with Source-Skin-Distance (SSD) is also studied. Results show an underestimation of the measured out-of-field dose in the calculated values for each of large field size (5.2% instead of 7.3% at field size of 30 × 30 cm^2), energy of 15 MV (3.4% instead of 1.4%), collimator angle of 90º (3.4% instead of 1.3%) and small & large SSDs; 80 cm (2.7% instead of 1.1%) and 115 cm (3.6% instead of 1.1%). Therefore, when there are Organs at Risk (OARs) near to the field edge it is recommended to measure the out-of-field dose that reaches those OARs in order to accurately estimate their absorbed doses. This would probably help in the design of proper shields for such organs in order to protect them from a possible secondary cancer risk.

Keywords: ***Pinpoint; Out-of-field dose; Dosimetry; Radiotherapy***

Received Date: May 25, 2020; **Accepted Date:** June 13, 2020; **Published Date:** June 20, 2020

Introduction

The greatest challenge for radiation therapy is to attain the highest probability of cure with the least morbidity. The simplest way to increase this therapeutic ratio with radiation is to encompass all cancer cells with sufficient doses of radiation during each fraction, while simultaneously sparing surrounding normal tissues [1].

The protection of normal tissues can be performed by the collimation of radiation beam. For irregular radiation fields, either Cerrobend blocks [2] or Multi-Leaf Collimators (MLCs) can be used [3].

Citation: Ahmed M Abdelaal, Measured and Calculated Out-of-Field Dose Using Pinpoint Ionization Chamber Detector. J Med Biol 2(2): 82-89.

Three dimensional conformal radiotherapy treatment (3D CRT) is refers to the use of software and hardware tools through incorporation of anatomic information into the treatment planning process to design and implement more accurate and conformal radiation therapy that confined the radiation dose to planning target volume (PTV) [4,5].

The occurrence of secondary malignancies in patients treated with radiation was found to be maximum in the normal tissue surrounding the target where the highest dose was delivered [6]. An increased risk of cancer incidence after exposure to low doses has been previously reported [7,8].

An accurate assessment of the secondary cancer risk following a treatment with radiation requires a detailed knowledge of the dose profile outside the tumor [9].

In clinical photon beams, the dose outside the geometrical field limits is produced by photons originating from head leakage, scattering at the beam collimators and the flattening filter (head scatter) and scattering from the directly irradiated region of the patient or phantom [10].

TPSs are used to model treatment fields that deliver absorbed dose to a clinical target volume while minimizing the dose in normal tissues, ensuring dose is below population-based tolerance levels and avoiding non-target critical structures [11].

TPSs are modeling the treatment fields to deliver adequate dose to PTVs. Many planning algorithms are developed for accurate dose predication in field dosimetry, while out-of-field dose predictions are poor [12,13].

Dose calculations by a TPS may also be precluded by a lack of imaging information related to the organs in question: patients' CT scans typically include only the anatomy required for treatment planning and nearby organs or structures at risk, in keeping with the best practices of avoiding unnecessary exposure [14].

Materials and Methods

Characteristics of pinpoint detector

The pinpoint ionization chamber (model 31014, inner diameters of 2 mm, volume of 0.016 cm^3, PTW, Germany) can be used for depth dose, absolute dose and relative beam profile measurements in a motorized water phantom for characterization of linear accelerator radiation fields. The nominal energy range is ^{60}Co up to 50 MV photons. Flexible connection cable can be supplied with different connector types. The wall material is graphite with a protective acrylic cover.

Three dimensional water phantom

A Large size motorized 3D water phantom (Model MP3-M, with moving detector range of 60 × 50 × 40.7 cm^3, PTW, Germany). It includes a precision 3D stainless steel movement mechanism and three stepper motors for a detector positioning speed of 50 mm/s and a positioning accuracy of ± 0.1 mm. The tank is supplied with a quick release coupling to easily connect the water reservoir (Model T43163). The delivery includes a cable connection box mounted to the tank, a spirit level and an ion chamber-adjusting device. To operate the tank, MEPHYSTO software and an electronic system (TBA) are required. This phantom is used for automatic dose distribution measurements of radiation therapy beams.

Linear accelerator (Linac)

Linac of type a Siemens ONCOR is used in this study. In this linac, the MLC delivery system replaces the lower movable jaws inside head of the linear accelerator. It is a multi-energy machine (6 MV and 15 MV operating up to 500 MU/min and 6 electron energies). The OPTIFOCUS MLC for the ONCOR linear accelerators has 41 pairs of inner leaves with a 1.0 cm width that is projected at iso-center.

Treatment planning system (TPS)

XIO Treatment Planning System (version 4.6.2, Elekta, CMS, England) is used in the present work. It employs convolution, Clarkson and superposition algorithms in dose calculation for photon mode therapy and pencil beam algorithm in electron mode therapy. It uses a cumulative Dose-Volume Histogram (DVH) in the evaluation of plans. It has an Intensity Modulated Radiotherapy (IMRT) option that uses step and shoot method in treatment planning using inverse planning software. The leaf sequencer is used to convert an optimized fluence into a deliverable sequence of MLC segments.

Irradiation conditions

Field sizes ranging from 10 × 10 cm^2 to 30 × 30 cm^2 with increment of 10 cm^2 are used to perform the out-of-field dose measurements at SSD of 100 cm. Then measurements are performed with different SSDs ranging from 80 cm to 115 cm to evaluate the effect of SSD on the out-of-field dose. Measurements are carried out with energies of 6 MV and 15 MV to investigate the effect of energy on the out-of-field dose. The out-of-field dose is measured at distances ranging from 1cm to 12cm with increment of 1mm from the field edge along the x axis. The out-of-field dose is measured at collimator angles of 0° and 90° in order to evaluate the effect of MLCs and jaws on the out-of-field dose. The out-of-field dose is calculated as the percentage of dose on the central axis for each field size and depth to dose at a selected distance from field edge at D_{max}.

Calculated dose profiles are obtained from non-image patient study sets on TPS. The profile is sent in ASCII data format through a network to a dose profile folder in the TPS and compared to the measured profile using a Microsoft Excel data sheet. This allowed the evaluation of the percentage deviation of the calculated out-of-field dose from the measured one.

Results and Discussion

Measured and calculated out-of-field dose at different field sizes

Figure 1 shows the variation in measured and calculated out-of-field dose with distance to central axis for three different field sizes 10 × 10 cm^2, 20 × 20 cm^2 and 30 × 30 cm^2, respectively at a depth of 1.5 cm using pinpoint ionization chamber detector.

For the three given field sizes, the measured out-of-field dose exhibits higher values compared to calculated. This behaviour is more apparent for the 30 × 30 cm^2 field. The measured mean out-of-field dose also shows higher values compared to calculated values at all field sizes (Figure 2). Moreover, one can notice that there is always an increase in both measured and calculated mean out-of-field dose with field size. The measured mean out-of-field dose is constantly underestimated in the calculated values for all field sizes. The percentage underestimation ((measured-calculated)/calculated%) is 23% (2.6% instead of 3.2%) at field size of 10 × 10 cm^2 and increases to 40% (5.2% instead of 7.3%) at field size of 30 × 30 cm^2.

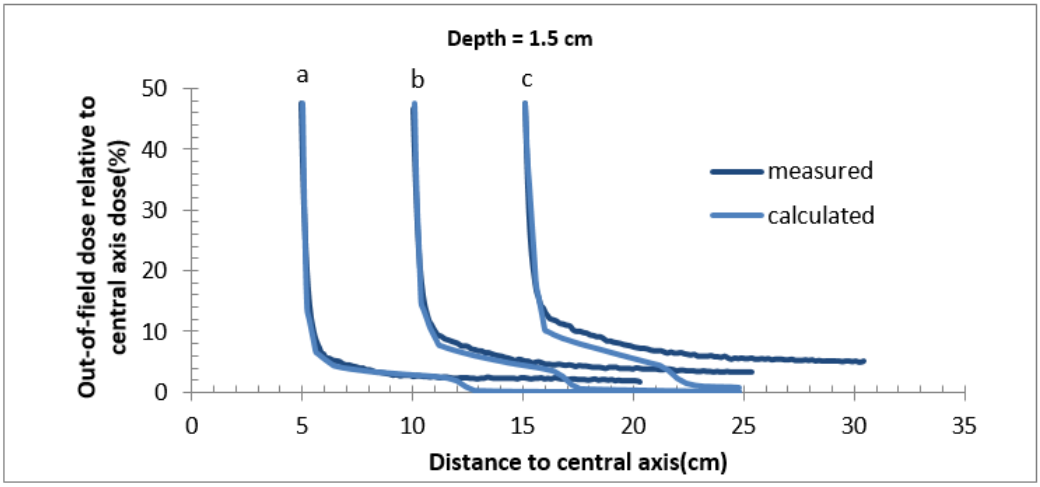

Figure 1: The variation in the measured and calculated out-of-field dose with distance to central axis for different field sizes, a: 10 × 10 cm^2, b: 20 × 20 cm^2 and c: 30 × 30 cm^2 using pinpoint ionization chamber detector.

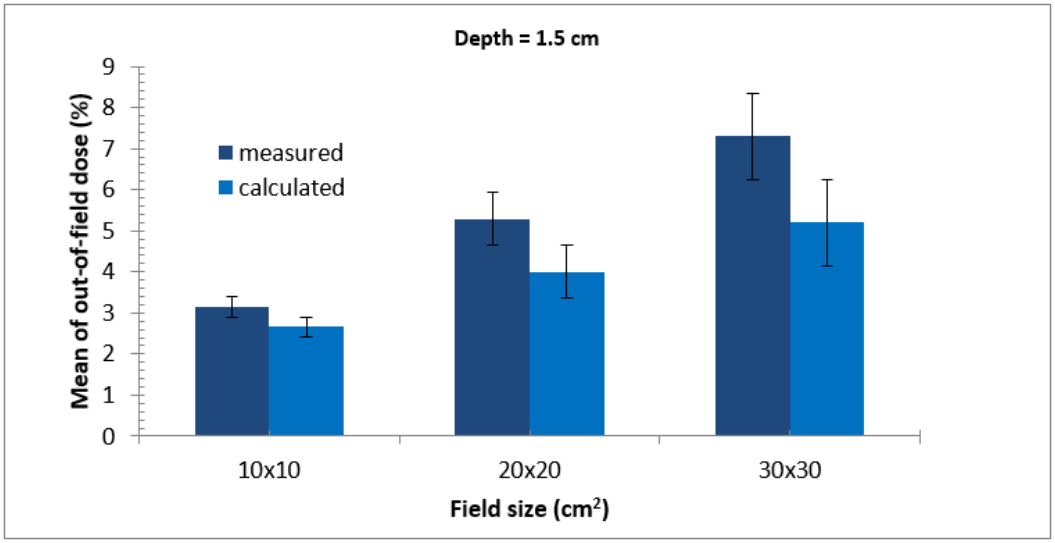

Figure 2: Variation of measured and calculated mean out-of-field dose with field size using pinpoint ionization chamber detector. The error bars represent the standard deviation (SD).

Measured and calculated out-of-field dose at different depths

Figure 3a & Figure 3b show an example of the variation in the measured and the calculated out-of-field dose with distance to central axis for field size of 10 × 10 cm^2 at two depths, (a) 1.5 cm and (b) 5 cm using Pinpoint ionization chamber detector.

Figure 4 shows Variation of measured and calculated mean out-of-field dose with depth using Pinpoint ionization chamber detector.

Similar to the variation with field size (section 3.1), there is greater measured mean out-of-field dose for all depths compared to calculated. The measured mean out-of-field dose is always underestimated in the calculated values for all depths. The percentage underestimation is 14% (2.7% instead of 3.1%) at depth of 1.5 cm and 2.4% (4.1% instead of 4.2%) at depth of 30 cm.

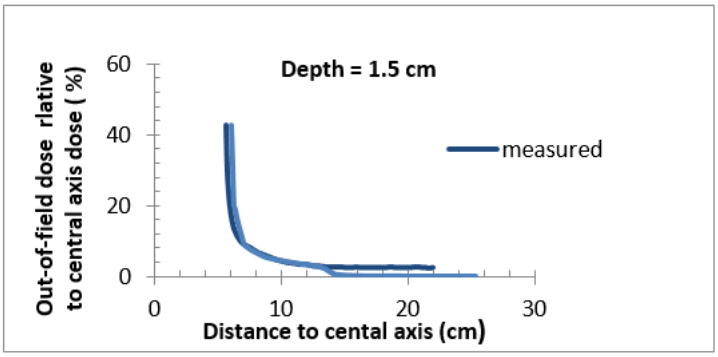

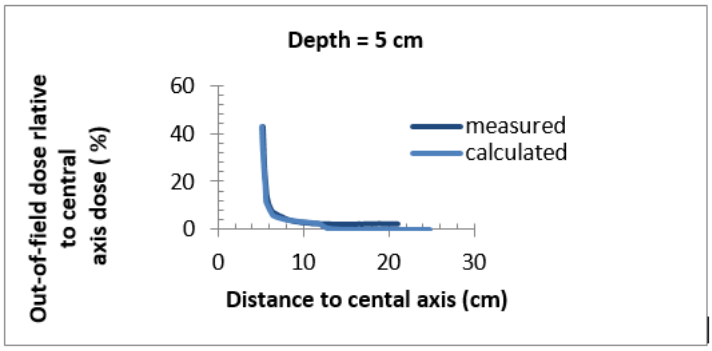

Figure 3a & Figure 3b: The variation in the measured and calculated out-of-field dose with distance to central axis for field size of 10 × 10 cm^2 at depth of 1.5 cm using Pinpoint ionization chamber detector. The variation in the measured and calculated out-of-field dose with distance to central axis for field size 10 × 10 cm^2 at depth of 5 cm using pinpoint ionization chamber detector.

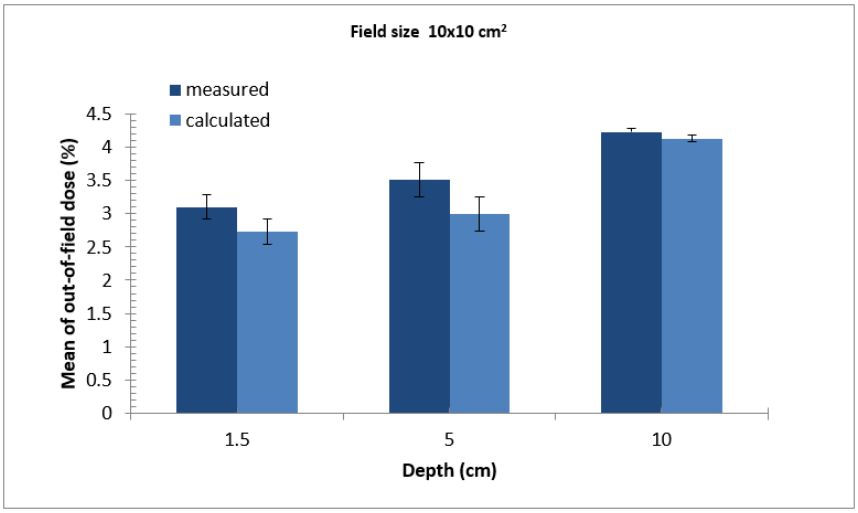

Figure 4: Variation of measured and calculated mean out-of-field dose with depth using Pinpoint ionization chamber detector.

Measured and calculated out-of-field dose at different beam energies

Table 1 summarizes the variation in the values of measured and calculated mean out-of-field dose with beam energy (6 MV and 15 MV) for field size of 10 × 10 cm^2, at a depth of 1.5 cm using pinpoint ionization chamber detectors.

Mean out-of-field dose		
	Measured (%) using pinpoint	Calculated (%) using TPS
6 MV	3.2	2.6
15 MV	3.4	1.4

Table 1: Summary of the variation in measured (using Pinpoint and Semiflex detectors) and calculated (using TPS) mean out-of-field dose values at two energies (6 MV and 15 MV) for field size of 10 × 10 cm^2, at a depth of 1.5 cm.

From Table 1, one can observe that, at 6 MV and 15 MV, the calculated values underestimate the out-of-field dose measured using the Pinpoint ionization chamber detector. This underestimation of the out-of-field dose is more apparent at the higher energy (15 MV).

Measured and calculated out-of-field dose at different collimator angles

Table 2 shows the variation in the values of measured (using pinpoint ionization chamber detector) and calculated (using TPS) mean out-of-field dose with collimator angles 0º and 90º for field size of 10 × 10 cm^2, at a depth of 1.5 cm and energy of 6 MV.

Mean out-of-field dose		
	Measured (%) using pinpoint	Calculated (%) using TPS
Collimator 0º	3.2	2.6
Collimator 90º	3.4	1.3

Table 2: Summary of the variation in measured (using pinpoint and ionization chamber detectors) and calculated (using TPS) mean out-of-field dose values at two different collimator angles (0º and 90º).

From Table 2, one can observe that at 0º and 90º collimator angles, the calculated value underestimates the out-of-field dose measured using the pinpoint ionization chamber detector. This underestimation of the out-of-field dose is more apparent at 90º collimator angle.

Measured and calculated out-of-field dose at different Source-Skin-Distances (SSDs)

Table 3 presents the variation in mean measured and calculated out-of-field dose values at three different SSDs (80 cm, 100 cm and 115 cm) for field size of 10 × 10 cm^2 at a depth of 1.5 cm and energy of 6 MV using Pinpoint and ionization chamber detector.

Mean out-of-field dose		
	Measured (%) using pinpoint	Calculated (%) using TPS
SSD 80	2.7	1.1
SSD 100	3.2	2.6
SSD 115	3.6	1.1

Table 3: The variation in mean measured and calculated out-of-field dose values at three different SSDs (80 cm, 100 cm and 115 cm) for field size of 10 × 10 cm^2 at a depth of 1.5 cm and energy of 6 MV using pinpoint and semiflex ionization chamber detectors.

From Table 3 one can observe that at SSD of 80 cm, 100 cm and115 cm, the calculated values underestimate the out-of-field dose measured using pinpoint detector. This underestimation is more apparent at SDDs of 80 cm and 115 cm.

It should be noted that, for the results presented in this section, the underestimation and overestimation of measured out-of-field dose in the calculated values can be explained knowing that the TPS is generally commissioned using data that extends only few centimetres beyond the field edge. The dose beyond this field is not incorporated in the dose calculation. Therefore the ability of TPS to predict the dose out-side the treatment field is fairly poor [13,15-17].

To sum up, there is a repetitive observed underestimation of the measured out-of-field dose in the calculated values with each of large field size (5.2% instead of 7.3% at field size of 30 × 30 cm^2), energy 15 MV (3.4% instead of 1.4%), collimator angle of 90º (3.4% instead of 1.3%) and small & large SSDs; 80 cm (2.7% instead of 1.1%) and 115 cm (3.6% instead of 1.1%). Therefore, one has to consider these parameters during the planning of a patient, especially when there are OARs near to the field edge. In this case it is recommended to measure the out-of-field dose that reaches those OARs in

order to protect such organs from a possible secondary cancer risk. The secondary cancer risk can be calculated simply by multiplying the measured doses by the nominal cancer risk coefficients of each organ [18]. If the out-of -field dose relative to the central axis dose of the treatment fields is large enough to induce secondary cancer, proper shields should be used in order to protect those organs [19].

Conclusion

There is a repetitive observed underestimation of the measured out-of-field dose in the calculated values using pinpoint ionization chamber detector in the measurement, this underestimation is more apparent with each of large field size, energy 15 M, collimator angle of 90° and small (80 cm) & large SSDs (115 cm). Therefore, one has to consider these parameters during the planning of a patient, especially when there are OARs near to the field edge.

References

1. Bucci MK, Bevan A, Roach III M (2005) Advances in radiation therapy: Conventional to 3D, to IMRT, to 4D, and beyond. CA: A Cancer Journal for Clinicians 55(2): 117-134.
2. Wojcicka JB, Yankelevich R, Werner BL, et al. (2008) Technical note: On cerrobend shielding for 18-22MeV electron beams. Medical physics 35(10): 4625-4629.
3. Hogstrom KR, Boyd RA, Antolak JA, et al. (2004) Dosimetry of a prototype retractable eMLC for fixed-beam electron therapy. Medical Physics 31(3): 443-462.
4. Marks LB, Bentel G, Light K, et al. (2000) Routine 3D treatment planning: Opportunities, challenges, and hazards. Oncology-Williston Park Then Huntington 14(8): 1191-1200.
5. Klein EE, Maserang B, Wood R, et al. (2006) Peripheral doses from pediatric IMRT. Medical Physics 33(7 Part1): 2525-2531.
6. Dörr W, Herrmann T (2002) Cancer induction by radiotherapy: Dose dependence and spatial relationship to irradiated volume. Journal of Radiological Protection 22(3A): A117.
7. Pierce DA, Preston DL (2000) Radiation-related cancer risks at low doses among atomic bomb survivors. Radiation Research 154(2): 178-186.
8. Preston DL, Shimizu Y, Pierce DA, et al. (2003) Studies of mortality of atomic bomb survivors. Report 13: Solid cancer and noncancer disease mortality: 1950–1997. Radiation Research 160(4): 381-407.
9. Xu XG, Bednarz B, Paganetti H (2008) A review of dosimetry studies on external-beam radiation treatment with respect to second cancer induction. Physics in Medicine & Biology 53(13): R193.
10. Chofor N, Harder D, Willborn KC, et al. (2012) Internal scatter, the unavoidable major component of the peripheral dose in photon-beam radiotherapy. Physics in Medicine & Biology 57(6): 1733.
11. Bentzen SM, Constine LS, Deasy JO, et al. (2010) Quantitative analyses of normal tissue effects in the clinic (QUANTEC): An introduction to the scientific issues. International Journal of Radiation Oncology* Biology* Physics 76(3): S3-S9.
12. Jang SY, Liu HH, Mohan R (2008) Underestimation of low-dose radiation in treatment planning of intensity-modulated radiotherapy. International Journal of Radiation Oncology* Biology* Physics 71(5): 1537-1546.
13. Kaderka R, Schardt D, Durante M, et al. (2012) Out-of-field dose measurements in a water phantom using different radiotherapy modalities. Physics in Medicine & Biology 57(16): 5059.

14. Goske MJ, Applegate KE, Boylan J, et al. (2008) The image gently campaign: Working together to change practice. American Journal of Roentgenology 190(2): 273-274.
15. Das IJ, Cheng CW, Watts RJ, et al. (2008) Accelerator beam data commissioning equipment and procedures: Report of the TG-106 of the therapy physics committee of the AAPM. Medical Physics 35(9): 4186-4215.
16. Taylor ML, Kron T (2011) Consideration of the radiation dose delivered away from the treatment field to patients in radiotherapy. Journal of Medical Physics/Association of Medical Physicists of India 36(2): 59.
17. Scarboro SB, Stovall M, White A, et al. (2010) Effect of organ size and position on out-of-field dose distributions during radiation therapy. Physics in Medicine & Biology 55(23): 7025.
18. Sungkoo CHO, Seong Hoon KIM, Chan Hyeong KIM, et al. (2011) Secondary cancer risks in out-of-field organs for 3-D conformal radiation therapy. Progress in Nuclear Science and Technology 1: 512-524.
19. Atarod M, Shokrani P, Pourmoghadas A (2012) Design of a generally applicable abdominal shield for reducing fetal dose during radiotherapy of common malignancies in pregnant patients. International Journal of Radiation Research 10(3-4): 151-156.